Atty. Docket No: 2459-1-003

IN THE UNITED STATES PATENT AND TRADEMARK OFFICE

APPLICANT : Zhou, Ming-Ming *et al.*

SERIAL NO. : 09/510,314 EXAMINER: Lucas, Zachariah

FILED : February 22, 2000 ART UNIT: 1648

FOR : METHODS OF IDENTIFYING MODULATORS OF BROMODOMAINS

Certificate of Mailing Under 37 CFR 1.8

I hereby certify that this correspondence is being deposited with the United States Postal Service as first class mail in an envelope addressed to COMMISSIONER FOR PATENTS, P.O. BOX 1450, ALEXANDRIA, VA 22313-1450 May 26, 2010.

Michele Hofherr
Name of Person Depositing Mail)

Michele Hofherr 5.26.10
(Signature and Date)

DECLARATION UNDER 37 C.F.R. §1.131

COMMISSIONER FOR PATENTS
P.O. BOX 1450
ALEXANDRIA, VA 22313-1450

Dear Sir:

I, Ming-Ming Zhou, hereby declare as follows:

1. I am a Professor and Chairman of the Department of Structural and Chemical Biology at Mt. Sinai School of Medicine, a Director in the Translational Chemical Biology Center, and Co-Director of the Experimental Therapeutics Institute at Mount Sinai School of Medicine, having received my Ph.D. degree in Chemistry from Purdue University in 1993. After that, I served as a postdoctoral fellow at Abbott Laboratories in Chicago, Illinois.

2. My curriculum vitae is attached hereto as Exhibit A.

3. My principal area of research is Structural and Chemical Biology, as well as epigenetic regulation of gene transcription. Among other positions I serve as reviewer in numerous scientific journals including *Analytic Biochemistry, Biophysical Journal, Cell, Chemistry & Biology, EMBO Journal, European Journal of Biochemistry, FEBS Letters, GENE, JACS, Journal of Molecular Biology, Molecular Cell, Nature Structure & Molecular Biology, Protein Science, Science* and *Structure*. I also have served as a reviewer for funding agencies including the American Cancer Society, the American Heart Association, the Israel Science Foundation, the National Science Foundation, the NIH and the European Commissions.

4. I am an inventor of the above-referenced application together with Aneel Aggarwal, Ph.D.

5. That the subject application was filed in the United States Patent and Trademark Office on February 22, 2000.

6. I am also familiar with the scientific publication Dhalluin *et al., Nature* 1999; 399:491-496, which describes a research study that I directed in my research laboratory at Mount Sinai School of Medicine, and for which I served as a corresponding author and communicated with the editors of *Nature* for its publication.

7. The invention described and claimed in the above-referenced application was conceived in the United States prior to the effective date of Dhalluin *et al., Nature* 1999; 399:491-496. (June 3, 1999), particularly prior to March 29, 1999, the date that we submitted a revised manuscript to *Nature* for review. (*See*, attached copy of the revised manuscript, submitted herewith as Exhibit B).

8. I and co-inventor Aneel Aggarwal, Ph.D. were diligent in reducing the invention to practice at a minimum by filing United States Patent Application Serial No. 09/510,314, on February 22, 2000, from a date at least as early as December 7, 1998 when we completed the determination of the human PCAF bromodomain structure and identified its biochemical function as an acetyl-lysine binding domain. (*See*, attached copy of the Statistics Tables of the final family of the NMR solution structures of the PCAF bromodomain, submitted herewith as

Exhibit C).

9. As noted in paragraphs 7 and 8, I submit herewith as Exhibit B a copy of the revised manuscript submitted to the journal of *Nature* dated March 29, 1999, and copies of computer print-outs of the Statistics Tables of the NMR solution structures of the PCAF bromodomain dated December 8, 1998. The subject matter of the revised manuscript is identical to the reference Dhalluin *et al., Nature* 1999; 399:491-496. (June 3, 1999).

10. I further hereby declare that all statements made herein of my own knowledge are true and that all statement made on information and belief are believed to be true; and further that these statements were made with the knowledge that willful false statements and the like so made are punishable by fine or imprisonment, or both, under Section 1001 of Title 18 of the United States Code; and that such willful false statements may jeopardize the validity of the application, any patent issuing thereon, or any patent to which this verified statement is directed.

Dated: _____

_____

Ming-Ming Zhou, Ph.D.

EXHIBIT "B"

Revision / Nature
3/29/99

Structure and Ligand of a Histone Acetyltransferase Bromodomain

Christophe Dhalluin*, Justin Carlson*, Lei Zeng, Cheng He, Aneel K. Aggarwal, Ming-Ming Zhou

Structural Biology Program, Department of Physiology and Biophysics, Mount Sinai School of Medicine, New York, NY 10029-6574

* These authors contributed equally to the work.

Histone acetylation plays a pivotal role in chromatin remodeling and gene activation[1-4]. Notably, nearly all known histone acetyltransferase (HAT)-associated transcriptional coactivators contain bromodomains, which are ~110 amino-acid modules found in a large number of chromatin-associated proteins[5-9]. Despite the wide occurrence of bromodomains, their three-dimensional structure and binding partners remain unknown. Here we report the nuclear magnetic resonance (NMR) structure of the bromodomain from the HAT coactivator P/CAF (p300/CBP-associated factor)[10, 11]. The structure reveals an unusual left-handed up-and-down four-helix bundle. In addition, we show by a combination of structural and site-directed mutagenesis studies that bromodomains can interact specifically with acetylated-lysine, making them the first protein modules known to exhibit such interactions. The nature of acetyl-lysine recognition by the P/CAF bromodomain is similar to that of histone acetyltransferase interaction with acetyl-CoA. Together, these results functionally couple the bromodomain with the HAT activity of coactivators in the regulation of gene transcription.

The P/CAF bromodomain represents an extensive family of bromodomains (Fig. 1). A large number of long-range nuclear Overhauser enhancement (NOE)-derived distance restraints were identified in the NMR data of the P/CAF bromodomain, yielding a well-defined three-dimensional structure (Fig. 2a & b). The structure consists of a four-helix bundle (helices α_Z, α_A, α_B, and α_C) with a left-handed twist, and a long intervening loop between helices α_Z and α_A (termed the ZA loop) (Fig. 2c). The four amphipathic α-helices are packed tightly against one another in an antiparallel manner, with crossing angles for adjacent helices of ~16-20°. The up-and-down four-helix bundle can adapt two topological folds with opposite handedness (Fig. 2d). The right-handed four-helix bundle fold occurs more commonly and is seen in proteins such as hemerythrin and cytochrome b_{562}[12, 13]. The left-handed

fold of the bromodomain structure is less common, but also observed in proteins such as cytochrome b_5 and T4 lysozyme[12, 13]. This topological difference arises from the orientation of the loop between the first two helices (Fig. 2d). The right-handed four-helix bundle proteins have a relatively short hairpin-like connection between the first two helices, which makes the "preferred" turn to the right at the top of the first helix[12-14]. On the other hand, proteins with the left-handed fold usually have a long loop after the first helix and often contain additional secondary structural elements at the base of the helix bundle[12, 13]. In the bromodomain structure, this long ZA loop has a defined conformation and is packed against the loop between helices α_B and α_C (termed the BC loop) to form a hydrophobic pocket. These tertiary interactions between the two loops appear to favor the left turn of the ZA loop, resulting in the left-handed four-helix bundle fold of the bromodomain. The hydrophobic pocket formed by loops ZA and BC is lined by residues Val752, Ala757, Tyr760, Val763, Tyr802 and Tyr809 (Fig. 2e), and appears to be a site for protein-protein interactions (see below). The pocket is located at one end of the four-helix bundle, opposite to the N- and C-termini of the protein. Interestingly, the ZA loop varies in length amongst different bromodomains, but almost always contains residues corresponding to Phe748, Pro751, Pro758, Tyr760, and Pro767 (Fig. 1). The conservation of these residues within the ZA loop as well as residues within the α-helical regions implies a similar left-handed four-helix bundle structure for the large family of bromodomains (Fig. 1).

The modular bromodomain structure supports the idea that bromodomain can act as a functional unit for protein-protein interactions[6]. The observation that bromodomains are found in nearly all known nuclear HATs (A-type) that are known to promote transcription-related acetylation of histones on

specific lysine residues, but not present in cytoplasmic HATs (B-type)[7, 8, 15, 16], prompted us to explore whether bromodomains can interact with acetyl-lysine (AcK). We performed NMR titration of the P/CAF bromodomain with a peptide (SGRGKGG-AcK-GLGK) derived from histone H4, in which Lys8 is acetylated (Lys8 is the major acetylation site in H4 for GCN5, a yeast homologue of P/CAF[1, 17]). Remarkably, we found that the bromodomain could indeed bind the AcK peptide. Moreover, this interaction appeared to be specific, based on the ^{15}N-HSQC spectra which showed that only a limited number of residues underwent chemical shift changes as a function of peptide concentration (Fig. 3a). Conversely, NMR titration of the bromodomain with a non-acetylated, but otherwise identical H4 peptide, showed no noticeable chemical shift changes, demonstrating that the interaction between the bromodomain and the lysine-acetylated H4 peptide was dependent upon acetylation of lysine. The dissociation constant (K_D) for the AcK peptide was estimated to be 346 ± 54 μM. This binding is likely reinforced through additional interactions between bromodomain-containing proteins and target proteins. Notably, many chromatin-associated proteins contain two or multiple bromodomains (Fig. 1)[6]. Indeed, we also observed binding with another lysine-acetylated peptide (RKSTGG-AcK-APRKQ) derived from the major acetylation site on histone H3 (residues 9-20)[17] (data not shown). Together, these data show that the P/CAF bromodomain has the ability to bind AcK peptides in an acetylation dependent manner.

Intriguingly, the bromodomain residues that exhibited the most significant ^{1}H and ^{15}N chemical shift changes on peptide binding are located near the hydrophobic pocket between the ZA and BC loops (Fig. 3b). Because a similar pattern of amide chemical shift changes was observed with the two different

AcK-containing peptides, we surmised that the hydrophobic cavity is the primary binding site for AcK. This hypothesis was further supported by titration with acetyl-histamine, which mimics the chemical structure of the AcK side-chain (Fig. 3c). Both ^{15}N- and ^{13}C-HSQC spectra showed that interaction with acetyl-histamine was also acetylation-dependent, involving the same set of residues that showed chemical shift perturbations with similar concentration dependence (data not shown). It should be noted that the bromodomain did not bind to the amino acids acetyl-lysine or acetyl-histidine alone, possibly because of the presence of the charged amino, carboxyl, or caboxylate group adjacent to the acetyl moiety (Fig. 3c). Taken together, these results strongly suggest that the P/CAF bromodomain can interact with acetyl-lysine-containing proteins in a specific manner, and that this interaction is localized to the bromodomain hydrophobic cavity.

To identify the key residues involved in bromodomain-AcK recognition, we elucidated the NMR structure of the P/CAF bromodomain in complex with acetyl-histamine. As anticipated, the acetylated moiety binds in the bromodomain hydrophobic pocket (Fig. 4). The intermolecular interactions are largely hydrophobic in nature, with the methyl group of acetyl-histamine making extensive contacts with the side-chains of Val752, Ala757, and Tyr760, and the methylene groups of acetyl-histamine displaying specific NOEs to Val752, Ala757, Tyr760, Tyr802, and Tyr809. No intermolecular NOEs were observed for the imidazole ring of acetyl-histamine. From the spectral analysis it is clear that the structure of the bromodomain is very similar in both the free and complex forms.

It is worth noting that the bromodomain-AcK recognition is reminiscent of the interactions between the histone acetyltransferase Hat1 and acetyl-CoA[18]. Although the binding pockets of these two

otherwise structurally unrelated proteins are composed of different secondary structural elements, the nature of acetyl-lysine recognition has striking similarities. In particular, Tyr809, Tyr802, Tyr760, and Val752 in the bromodomain appear to be related to Phe220, Phe261, Val254, and Ile217 of Hat1, respectively, in their interactions with the acetyl moiety. This observation may suggest an evolutionary convergent mechanism of acetyl-lysine recognition between bromodomains and histone acetyltransferases.

To determine the relative contributions of residues within the hydrophobic cavity in bromodomain-AcK binding, we used site-directed mutagenesis to alter residues Tyr809, Tyr802, Tyr760, and Val752 (Table 1). Substitution of Ala for Tyr809 completely abrogated the bromodomain binding to the lysine-acetylated H4 peptide, while the Tyr802Ala, Tyr760Ala, and Val752Ala mutants had significantly reduced ligand binding affinity. To assess whether these mutations disrupted the overall bromodomain fold, we compared the ^{15}N-HSQC spectra of the mutants to that of the wild-type protein. For the Tyr809Ala mutant, the amide chemical shifts were only affected for a few residues near the mutation site. However, mutations of the other residues in the hydrophobic binding pocket perturbed the local protein conformation to greater extents, particularly the ZA loop (Table 1). Thus, the NMR structural analysis and the mutagenesis studies show that Tyr809, which is structurally supported by Trp746 and Asn803 (Fig. 4), is essential for the bromodomain interaction with the acetyl group of acetyl-lysine, while residues of Tyr802, Tyr760, and Val752 likely play both structural and functional roles in the recognition. These residues are highly conserved throughout the bromodomain family (Fig. 1), suggesting that recognition of acetyl-lysine may be a feature of bromodomains, in general.

In conclusion, our structural and mutagenesis results strongly implicate the bromodomains as acetyl-lysine binding domains, making them the first protein modules to exhibit such interactions. Like other modular domains, such as Src homology-2 (SH2) and phosphotyrosine binding (PTB) domains[19], which specifically interact with phosphotyrosine-containing proteins, the bromodomain/acetyl-lysine recognition could provide a means to regulate protein-protein interactions via protein lysine acetylation. In particular, our finding may explain the results of previous deletion experiments which showed that the bromodomain is indispensable for the function of GCN5 in yeast[20], and supports the hypothesis that bromodomains could contribute to highly specific histone acetylation by tethering transcriptional HATs to specific chromosomal sites[1]. Moreover, bromodomain-AcK binding could also be important for the assembly and activity of multiprotein complexes in transcriptional activation. The results reported here form the foundation for identifying specific biological ligands and for defining the molecular mechanisms by which the extensive family of bromodomains participate in chromatin remodeling and transcriptional activation.

Methods

Sample preparation. The bromodomain of P/CAF (residues 719-832) was subcloned into the pET14b expression vector (Novagen) and expressed in *Escherichia coli* BL21(DE3) cells. Uniformly ^{15}N- and $^{15}N/^{13}C$-labelled proteins were prepared by growing bacteria in a minimal medium containing $^{15}NH_4Cl$ with or without $^{13}C_6$-glucose. A uniformly $^{15}N/^{13}C$-labelled and fractionally deuterated protein sample was prepared by growing the cells in 75% ^2H_2O. The bromodomain was purified by affinity chromatography on a nickel-IDA column (Invitrogen) followed by the removal of poly-His tag by thrombin cleavage. The final purification of the protein was achieved by size-exclusion chromatography. The acetyl-lysine-containing peptides were prepared on a MilliGen 9050 peptide synthesizer (Perkin Elmer) using Fmoc/HBTU chemistry. Acetyl-lysine was incorporated using the reagent Fmoc-Ac-Lys with HBTU/DIPEA activation. NMR samples contained ~1mM protein in 100mM phosphate buffer of pH 6.5 and 5mM perdeuterated DTT and 0.5mM EDTA in $H_2O/^2H_2O$ (9/1) or ^2H_2O.

NMR spectroscopy. All NMR spectra were acquired at 30°C on a Bruker DRX600 or DRX500 spectrometer. The backbone assignments of the ^1H, ^{13}C, and ^{15}N resonances were achieved using deuterium-decoupled triple-resonance experiments of HNCACB and HN(CO)CACB[21] recorded using the uniformly $^{15}N/^{13}C$-labelled and fractionally deuterated protein. The side-chain atoms were assigned from 3D HCCH-TOCSY[22] and (H)C(CO)NH-TOCSY[23] data collected on the uniformly $^{15}N/^{13}C$-labelled protein. Stereospecific assignments of methyl groups of the Val and Leu residues were obtained using a fractionally ^{13}C-labelled sample[24]. The NOE-derived distance restraints were obtained from ^{15}N- or ^{13}C-edited 3D NOESY spectra[22]. ϕ-angle restraints were determined based on the $^3J_{HN,H\alpha}$ coupling

constants measured in a 3D HNHA spectrum[22]. Slowly exchanging amide protons were identified from a series of 2D ^{15}N-HSQC spectra recorded after the H_2O buffer was changed to a ^2H_2O buffer. The intermolecular NOEs used in defining the structure of the bromodomain/Ac-histamine complex were detected in ^{13}C-edited (F_1), ^{13}C/^{15}N-filtered (F_3) 3D NOESY spectrum[22]. All NMR spectra were processed with the NMRPipe/NMRDraw programs and analyzed using NMRView[25].

Structure calculations. Structures of the bromodomain were calculated with a distance geometry/simulated annealing protocol using the X-PLOR program[26]. A total of 1324 manually assigned NOE-derived distance restraints were obtained from the ^{15}N- and ^{13}C-edited NOE spectra. Further analysis of the NOE spectra was carried out by the iterative automated assignment procedure using ARIA[27], which integrates with X-PLOR for structure calculations. A total of 1519 unambiguous and 590 ambiguous distance restraints were identified from the NOE data by ARIA, many of which were checked and confirmed manually. The ARIA-assigned distance restraints were in agreement with the structures calculated using only the manually assigned NOE distance restraints, 28 hydrogen-bond distance restraints for 14 hydrogen bonds, and 54 ϕ-angle restraints. The final structure calculations employed a total of 3515 NMR experimental restraints obtained from the manual and the ARIA-assisted assignments, 2843 of which were unambiguously assigned NOE-derived distance restraints that comprise of 1077 intra-residue, 621 sequential, 550 medium-range, and 595 long-range NOEs. For the ensemble of the final 30 structures, no distance and torsional angle restraints were violated by more than 0.3Å and 5°, respectively. The total, distance violation, and dihedral violation energies were 178.7 ± 2.4 kcal mol^{-1}, 41.6 ± 0.9 kcal mol^{-1}, and 0.50 ± 0.06 kcal mol^{-1}, respectively. The Lennard-Jones potential

which was not used during any refinement stage, was -526.2 ± 16.8 kcal mol^{-1} for the final structures. Ramachandran plot analysis of the final structures (residues 727-828) with Procheck-NMR[28] showed that 71.0 ± 0.6%, 23.8 ± 0.6%, 3.5 ± 0.2%, and 1.7 ± 0.2% of the non-Gly and non-Pro residues were in the most favorable, additionally allowed, generously allowed, and disallowed regions, respectively. The corresponding values for the residues in the four α-helices (residues 727-743, 770-776, 785-802, and 807-827) were 88.9 ± 0.4%, 11.0 ± 0.4%, 0.1 ± 0.1%, and 0.0 ± 0.0%, respectively. The structure of the bromodomain/Ac-histamine complex was determined using the free form structure and additional 25 intermolecular and 5 intra-ligand NOE-derived distance restraints.

Site-directed mutagenesis. Mutant proteins were prepared using the QuickChange site-directed mutagenesis kit (Stratagene). The presence of appropriate mutations was confirmed by DNA sequencing.

Ligand titration. Ligand titration experiments were performed by recording a series of 2D ^{15}N- and ^{13}C-HSQC spectra on the uniformly ^{15}N-, and $^{15}N/^{13}C$-labelled bromodomain (~0.3mM), respectively, in the presence of different amounts of ligand concentration ranging from 0 to ~2.0mM. The protein sample and the stock solutions of the ligands were all prepared in the same aqueous buffer containing 100mM phosphate and 5mM perdeuterated DTT at pH 6.5.

References

1. Brownell, J.E. & Allis, C.D. Special HATs for special occasions: Linking histone acetylation to chromatin assembly and gene activation. *Curr. Opin. Genet. Dev.* **6**, 176-184 (1996).

2. Grunstein, M. Histone acetylation in chromatin structure and transcription. *Nature* **389**, 349-352 (1997).

3. Wolffe, A.P. Sinful repression. *Nature* **387**, 16-17 (1997).

4. Shikama, N., Lyon, J. & Thangue, N.B.L. The p300/CBP family: Integrating signals with transcription factors and chromatin. *Trends Cell Biol.* **7**, 230-236 (1997).

5. Haynes, S.R., *et al.* The bromodomain: A conserved sequence found in human, *Drosophia* and yeast proteins. *Nucleic Acids Res.* **20**, 2603-2603 (1992).

6. Jeanmougin, F., Wurtz, J.M., Douarin, B.L., Chambon, P. & Losson, R. The bromodomain revisited. *Trends Biochem. Sci.* **22**, 151-153 (1997).

7. Brownell, J.E., *et al.* Tetrahymena histone acetyltransferase A: A homolog to yeast Gcn5p linking histone acetylation to gene activation. *Cell* **84**, 843-851 (1996).

8. Ogryzko, V.V., Schiltz, O.L., Russanova, V., Howard, B.H. & Nakatani, Y. The transcriptional coactivators p300 and CBP are histone acetyltransferases. *Cell* **87**, 953-959 (1996).

9. Bannister, A.J. & Kouzarides, T. The CBP co-activator is a histone acetyltransferase. *Nature* **384**, 641-643 (1996).

10. Yang, X.-J., Ogryzko, V.V., Nishikawa, J.-I., Howard, B.H. & Nakatani, Y. A p300/CBP-associated factor that competes with the adenoviral oncoprotein E1A. *Nature* **382**, 319-324 (1996).

11. Puri, P.L., *et al.* Differential roles of p300 and PCAF acetyltransferases in muscle differentiation. *Cell* **1**, 35-45 (1997).

12. Richardson, J.S. The anatomy and taxonomy of protein structure. *Adv. Protein Chem.* **34**, 167-339 (1981).

13. Presnell, S.R. & Cohen, F.E. Topological distribution of four-α-helix bundles. *Proc. Natl. Acad. Sci. USA* **86**, 6592-6596 (1989).

14. Weber, P.C. & Salemme, F.R. Structural and functional diversity in 4-α-helical proteins. *Nature* **287**, 82-84 (1980).

15. Kurokawa, R., *et al.* Differential use of CREB binding protein-coactivator complexes. *Nature* **279**, 700-703 (1998).

16. Chen, H., *et al.* Nuclear receptor coactivator ACTR is a novel histone acetyltransferase and forms a multimeric activation complex with P/CAF and CBP/p300. *Cell* **90**, 569-580 (1997).

17. Kuo, M.-H., *et al.* Transcription-linked acetylation by Gcn5p of histone H3 and H4 at specific lysines. *Nature* **383**, 269-272 (1996).

18. Dutnall, R.N., Tafrov, S.T., Sternglanz, R. & Ramakrishnan, V. Structure of the histone acetyltransferase Hat1: A paradigam for the GCN5-related N-acetyltransferase superfamily. *Cell* **94**, 427-438 (1998).

19. Pawson, T. Protein modules and signalling networks. *Nature* **373**, 573-580 (1995).

20. Georgakopoulos, T., Gounalaki, N. & Thireos, G. Gentic evidence for the interaction of the yeast transcriptional co-activator proteins GCN5 and ADA2. *Mol. Gen. Genet.* **246**, 723-728 (1995).

21. Yamazaki, T., Lee, W., Arrowsmith, C.H., Mahandiram, D.R. & Kay, L.E. A suite of triple resonance NMR experiments for the backbone assignment of ^{15}N, ^{13}C, ^{2}H labeled proteins with high sensitivity. *J. Am. Chem. Soc.* **116**, 11655-11666 (1994).

22. Clore, G.M. & Gronenborn, A.M. Multidimensional heteronuclear nuclear magnetic resonance of proteins. *Meth. Enzymol.* **239**, 249-363 (1994).

23. Logan, T.M., Olejniczak, E.T., Xu, R.X. & Fesik, S.W. A general method for assigning NMR spectra of denatured proteins using a 3D HC(CO)NH-TOCSY triple resonance experiments. *J. Biolmol. NMR* **3**, 225-231 (1993).

24. Neri, D., Szyperski, T., Otting, G., Senn, H. & Wüthrich, K. Stereospecific nuclear magnetic resonance assignments of the methyl groups of valine and leucine in the DNA-binding domain of the 434 repressor by biosynthetically directed fractional ^{13}C labeling. *Biochemistry* **28**, 7510-7516 (1989).

25. Johnson, B.A. & Blevins, R.A. NMRView: A computer program for the visualization and analysis of NMR data. *J. Biomol. NMR* **4**, 603-614 (1994).

26. Brünger, A.T. *X-PLOR Version 3.1: A system for X-Ray crystallography and NMR* (Yale University Press, New Haven, CT, 1993).

27. Nilges, M. & O'Donoghue, S. Ambiguous NOEs and automated NOE assignment. *Prog. NMR Spectroscopy* **32**, 107-139 (1998).

28. Laskowski, R.A., Rullmannn, J.A., MacArthur, M.W., Kaptein, R. & Thornton, J.M. AQUA and PROCHECK-NMR: Programs for checking the quality of protein structures solved by NMR. *J. Biomol. NMR* **8**, 477-486 (1996).

29. Carson, M. Ribbons 2.0. *J. Appl. Crystallogr.* **24**, 958-961 (1991).

30. Nicholls, A., Bharadwj, R. & Honig, B. GRASP: Graphical representation and analysis of surface properties. *Biophys. J.* **64**, 166-170 (1993).

Acknowledgements. We thank M. Sattler for providing NMR pulse sequences, M. Nilges and M. Rosen for advise on the ARIA/X-PLOR and NMRView programs, respectively, C. Escalante for advice on protein preparation, O. Plotnikova for assistance in the preparation of mutant proteins, I. Wolf for peptide synthesis, D. Logothetis, H. Weinstein, L. Shapiro, R. Margolskee, and A. Farooq for helpful suggestions and critical reading of the manuscript. This work was supported by discretionary funds from the Mount Sinai School of Medicine (to M.M.Z.) and NIH grants (to A.A.).

Correspondence and requests for materials should be addressed to M.M.Z. (e-mail: zhoum@inka.mssm.edu). Coordinates for the NMR structure of the P/CAF bromodomain have been deposited in the Brookhaven Protein Data Bank under accession code 1B91.

Table 1. Structural and Functional Analysis of the P/CAF Bromodomain Mutants

Bromodomain Proteins	Structural Integrity [a]	H4 AcK-Peptide Binding K_D (μM) [b]
Wild-Type	++++	346 ± 54
Tyr809Ala	++++	No Binding [c]
Tyr802Ala	+++	> 10,000 [d]
Tyr760Ala	+++	> 10,000
Val752Ala	++	> 10,000

a. The effects of mutations on the structural integrity of the bromodomain were assessed by using the ^{15}N-HSQC spectra. The amide ^{1}H/^{15}N resonances of the mutant proteins were compared to those of the wild-type bromodomain to determine if the particular mutations lead to global or local structure disruption. Severe line-broadening of the amide resonances would indicate protein conformational exchange due to a decrease of structure stability resulting from point mutations. Structural integrity of the mutant proteins is expressed here relative to that of the wild-type, using the signs of "++++" for as stable as the wild-type, "+++" for mildly destabilized, "++" for moderately destabilized, and "–" for completely unfolded.

b. The ligand binding affinity (K_D) of the bromodomain proteins was estimated by following chemical shift changes of amide peaks in the ^{15}N-HSQC spectra as a function of the ligand concentration.

c. No detectable ligand binding observed in the NMR titration.

d. Ligand binding affinity was significantly reduced and beyond the limit for reliable measurements by NMR titration.

Figure Legends

Figure 1. Structure-based sequence alignment of a selected number of bromodomains. The sequences were aligned based on the NMR-derived structure of the P/CAF bromodomain, and the predicated four α-helices are shown in green boxes. Bromodomains are grouped on the basis of the sequence and/or functional similarities as described in Ref. 7. Residue numbers of the P/CAF bromodomain are indicated above its sequence. Three absolutely conserved residues, corresponding to Pro751, Pro767, and Asn803 in the P/CAF bromodomain, are shown in red. Highly conserved residues are coloured in blue. The residues of the P/CAF bromodomain that interact with acetyl-histamine, as determined by intermolecular NOEs, are indicated by asterisks. The underlined residues were changed individually by site-directed mutagenesis to Ala. Genbank accession numbers are: *hsP/CAF* U57317, *hsGCN5* U57136, *ttP55* U47321, *scCGN5* Q03330, *hsP300* A54277, *hsCBP* S39162, *hsCCG1* P21675, *scBDF1* P35817, *ggPB1* X90849, *hsSNF2a* S45251, *hsBRG1* S39039, *mmTIF1a* S78219, *mmTIF1b* X99644.

Figure 2. Structure of the P/CAF bromodomain. **a,** Stereoview of the C_α trace of 30 superimposed NMR-derived structures of the bromodomain (residues 722-830). The N-terminal four residues (SKEP) which are structurally disordered are omitted for clarity. For the final 30 structures, the root-mean-square deviations (RMSDs) of the backbone and all heavy atoms are 0.63 ± 0.11Å and 1.15 ± 0.12Å for residues 723-830, respectively. The RMSDs of the backbone and all heavy atoms for the four α-helices (residues 727-743, 770-776, 785-802, and 807-827), are 0.34 ± 0.04Å and 0.87 ± 0.06Å, respectively. **b,** Stereoview of the bromodomain structures from the bottom of the protein, which is rotated ~90° from

the orientation in a. **c,** Ribbons[29] depiction of the averaged minimized NMR structure of the P/CAF bromodomain. The orientation of c is as shown in a. **d,** Schematic representation of the overall topology of the up-and-down four-helix bundle folds with the opposite handedness. The left-handed fold is seen in bromodomain, cytochrome b_5, and T4 lysozyme (left), whereas the right-handed four-helix bundles are observed in proteins such as hemerythrin and cytochrome b_{562} (right)[12, 13]. **e,** A molecular surface representation of the electrostatic potential (blue = positive; red = negative) of the bromodomain calculated in GRASP[30]. The hydrophobic and aromatic residues (Tyr809, Tyr802, Tyr760, Ala757, and Val752) located between the ZA and BC loops are indicated.

Figure 3. Binding of the P/CAF bromodomain to AcK. **a,** Superimposed region of the 2D ^{15}N-HSQC spectra of the bromodomain (~0.5mM) in its free form (red) and complexed to the AcK-containing H4 peptide (molar ratio 1:6) (black). **b,** Ribbon and dotted-surface diagram of the bromodomain depicting the location of the lysine-acetylated H4 peptide binding site. The colour coding reflects the chemical shift changes ($\Delta\delta$) of the backbone amide ^{1}H and ^{15}N resonances upon binding to the AcK peptide as observed in the ^{15}N-HSQC spectra. The normalized weighted average of the chemical shift changes was calculated by $\Delta_{av}/\Delta_{max} = [(\Delta\delta^2_{NH} + \Delta\delta^2_N/25)/2]^{1/2}/\Delta_{max}$, where Δ_{max} is the maximum weighted chemical shift difference observed for Tyr809 (0.16ppm). The backbone atoms are colour-coded in red, yellow, or green for residues that have Δ_{av}/Δ_{max} of >0.6 (Tyr809, Glu808, Asn803, and Ala757), 0.2-0.6 (Ala813, Tyr802, Tyr760, and Val752), or <0.2 (Cys812, Ser807, Cys799, Phe796, and Phe748), respectively. The non-perturbed residues are shown in blue. **c,** Chemical structures of acetyl-lysine, acetyl-histamine, and acetyl-histidine.

Figure 4. The acetyl-lysine binding pocket. Ribbons[29] depiction of a portion of the P/CAF bromodomain complexed with the acetyl-histamine. The ligand is colour-coded by atom type.

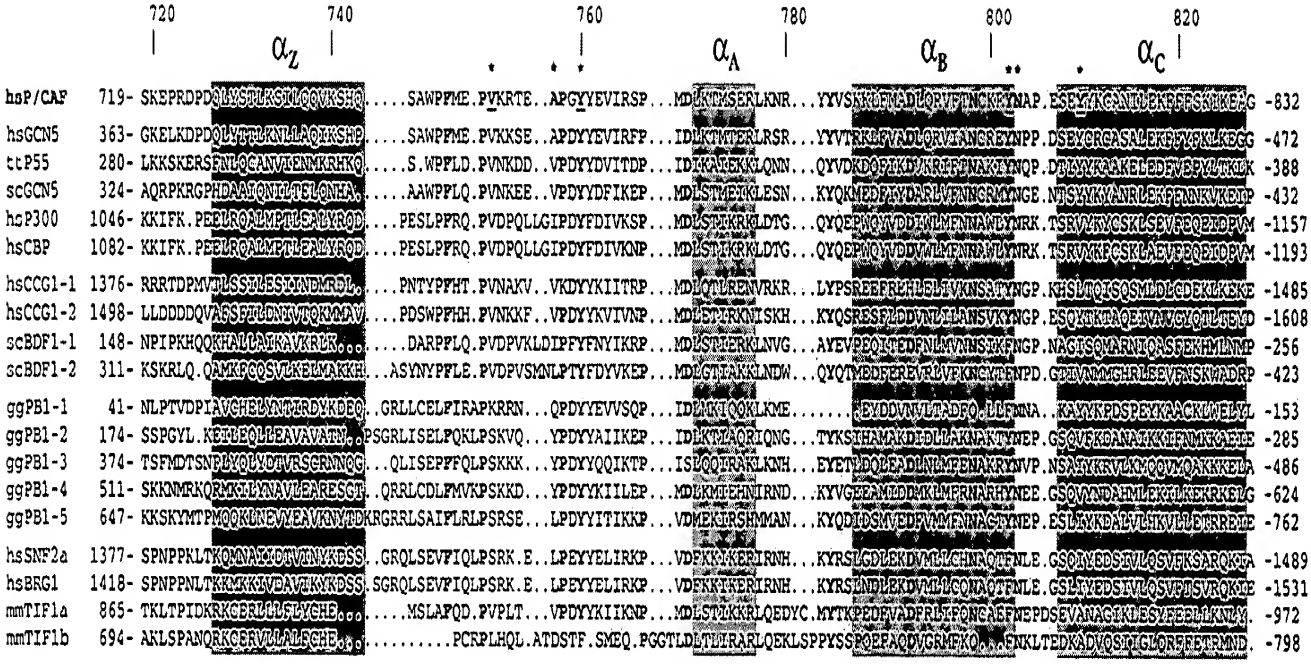
720
740
760
780
800
820
αZ
αA
αB
αC
hsP/CAF 719- SKEPRDPDQLYSTLKSTLQQVKSHQ.....SAWPFME.PVKRTE..APGYYEVIRSP...MDLKTMSERLKNR...YYVSKKEFMSDLQRVFTNCKTYNAP.ESEYYKCANILEKFFSSIKEYG -832
hsGCN5 363- GKELKDPDQLYTFLKNLLAQDKSHP.....SAWPFME.PVKKSE..APDYYEVIRFP...IDLKTMTERLRSR...YYVTRKEFVADLQRVIANCREYNPP.DSEYCRGASALEKFFVFSLKEGG -472
ttP55 280- LKKSKERSFNLQCANVIENMKRHKQ.....S.WPFLD.PVNKDD..VPDYYDVITDP...IDLKAIEKKLQNN...QYVDKDQFIKDVNRIFDNAKKYNQP.DTLYYKAAKELEDFVEPVLTKHK -388
scGCN5 324- AQRPKRGPHDAATQNLLTFLQNHA.....AAWPFLQ.PVNKEE..VPDYYDFIKEP...MDLSTMETKLESN...KYQKMEDFAYDARLVFNNCRMYNGE.NTSYYKYANRLEKFFNNKVKEIP -432
hsP300 1046- KKIFK.PEELRQALMPTLSALYRQD....PESLPFRQ.PVDPQLLGIPDYFDIVKSP...MDLSTIKRKLDTG...QYQEPWQYVDDVWLMFNNAWLYNRK.TSRVYKYCSKLSEVFEQEIDPVM -1157
hsCBP 1082- KKIFK.PEELRQALMPTLSALYRQD....PESLPFRQ.PVDPQLLGIPDYFDIVKNP...MDLSTIKRKLDTG...QYQEPWQYVDDVWLMFNNAWLYNRK.TSRVYKFCSKLAEVFEQEIDPVM -1193
hsCCG1-1 1376- RRRTDPMVTLSSTLESTINEMRDLQ....PNTYPFHT.PVNAKV..VKDYYKIITRP...MDLQTLRENVRKR...LYPSREEFEHHLELIVKNSATYNGP.KHSLTQISQSMLDLCDEKLKEKE -1485
hsCCG1-2 1498- LLDDDDQVASSPTLDNEVTQKMAV....PDSWPFHH.PVNKKF..VPDYYKVIVNP...MDLETIRKNISKH...KYQSRESFLDDVNLILANSVKYNGP.ESQVTKTAQEIYAVCVQTLTEVD -1608
scBDF1-1 148- NPIPKHQQKHALLAMKAVKRLKQQQ.....DARPFLQ.PVDPVKLDIPFYFNYIKRP...MDLSTMERKLNVG...AYEVPEQITEDFNLMVNNSIKFNGP.NAGISQMARNIQNSFEKHLNMP -256
scBDF1-2 311- KSKRLQ.QAMKPGQSVLKELMAKKH...ASYNYPFLE.PVDPVSMNLPTYFDYVKEP...MDLGTIAKKLNDW...QYQTMEDFERDVRLVFKNCMTFNPD.GDIVAMAGHRLEEVFNSKWADRP -423
ggPB1-1 41- NLPTVDPIAVCHELYNTIRDYKDEQ..GRLLCELFIRAPKRRN...QPDYYEVVSQP...IDLMTIQQKLKME.....PEYDDVNVLTADFQCLLFDNA..KAVYKFDSPEYKAACKLWELYL -153
ggPB1-2 174- SSPGYL.KELLEQLLEAVAVATL..PSGRLISELPQKLPSKVQ...YPDYYAIIKEP...IDLKTMAQRIQNG...TYKSIHAMAKDIDLLAKNAKTYNEP.GSQVFKDANTMKIFNMKKAELE -285
ggPB1-3 374- TSFMDTSNPLYQLVDTVRSGRNNQG...QLISEPFFQLPSKKK...YPDYYQQIKTP...ISLQQTRKKLKNH...EYETLDQLEADLNLMFENAKRYNVP.NSAIYKRVLKMQQVMQAKKKELA -486
ggPB1-4 511- SKKNMRKQRMKLLYNAVLEARESCT..QRRLCDLFMVKPSKKD...YPDYYKIILEP...MDLKMIEHNIRND...KYVGEEAMLDDMKMLFRNARHYNEE.GSQVVNDAHMLEKILKEKRKELG -624
ggPB1-5 647- KKSKYMTPMQQKLNEVVEAVKNYTDKRGRRLSAIFLRLPSRSE...LPDYYITIKKP...VDMEKIRSHMMAN...KYQDIDSMVEDFVMMFNNAGTYNEP.ESLLYKDALVLTKVLLDTRRELE -762
hsSNF2a 1377- SPNPPKLTKQMNAYLDTVDNYKDSS..GRQLSEVFIQLPSRK.E..LPEYYELIRKP...VDFKKIKERIRNH...KYRSLGDLEKDVMLLCHNAQTFNLE.GSQIYEDSIVLQSVFKSARQKTA -1489
hsBRG1 1418- SPNPPNLTKKMKKKIVDAVIKYKDSS.SGRQLSEVFIQLPSRK.E..LPEYYELIRKP...VDFKKIKERIRNH...KYRSLNDLEKDVMLLCQNAQTFNLE.GSLIYEDSIVLQSVFDSVRQKIE -1531
mmTIF1a 865- TKLTPIDKRKCERLLDLVGHE.....MSLAPQD.PVPLT...VPDYYKIIKNP...MDLSTMKKRLQEDYC.MYTKPEDFVADFRLIFDNCAEFNEPDSEVANAGIKLESYFEELLKNYY. -972
mmTIF1b 694- AKLSPANQRKCERVLLALSGHE.....PCRPLHQL.ATDSTF.SMEQ.PGGTLDLTLRARLQEKLSPPYSSPQEPAQDVGRMFKQAAENKLTEDKADVQSIQLGLQRFFTRMND. -798

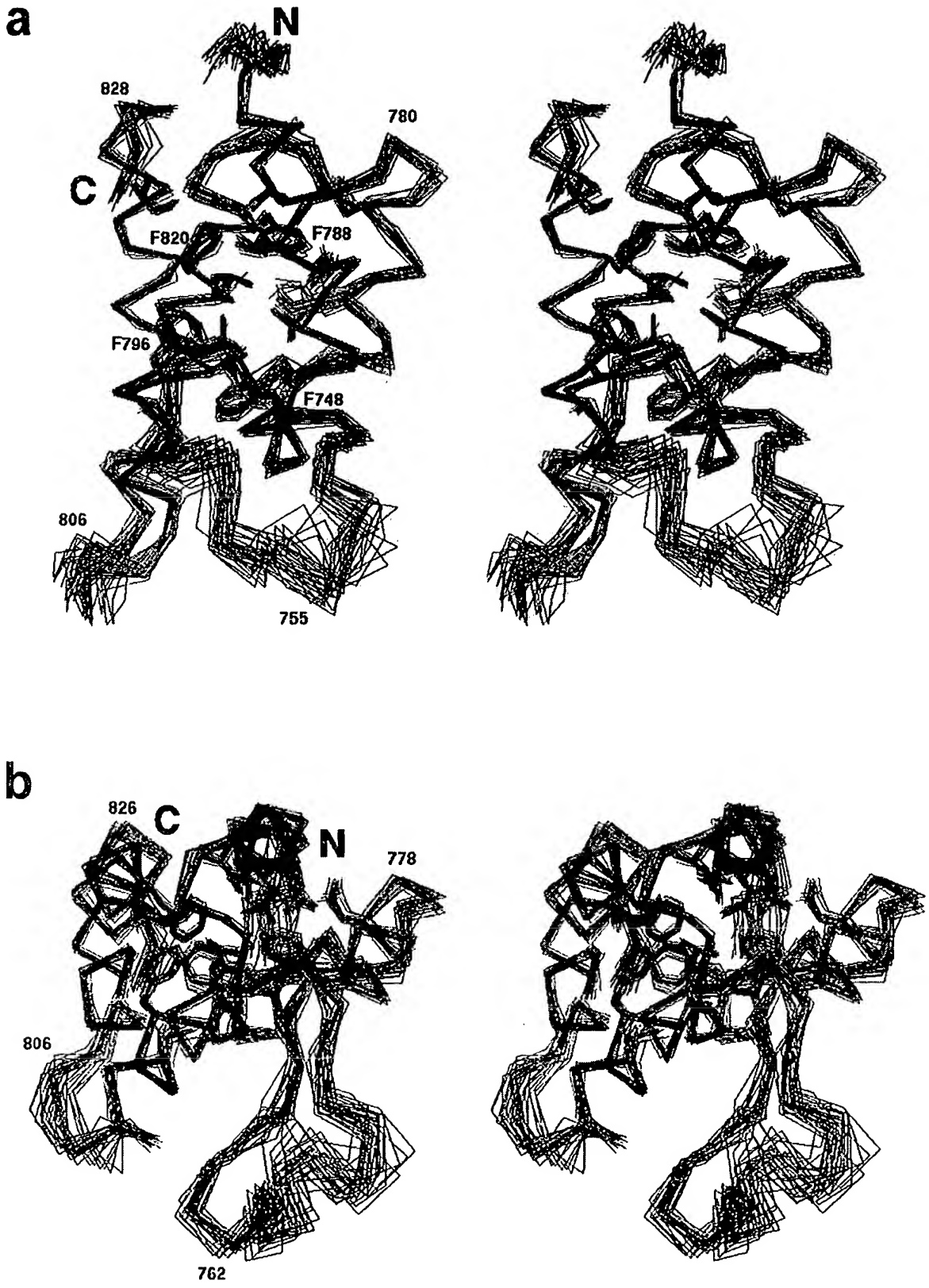
a
N
828
780
C
F820
F788
F796
F748
806
755
b
826
C
N
778
806
762

c

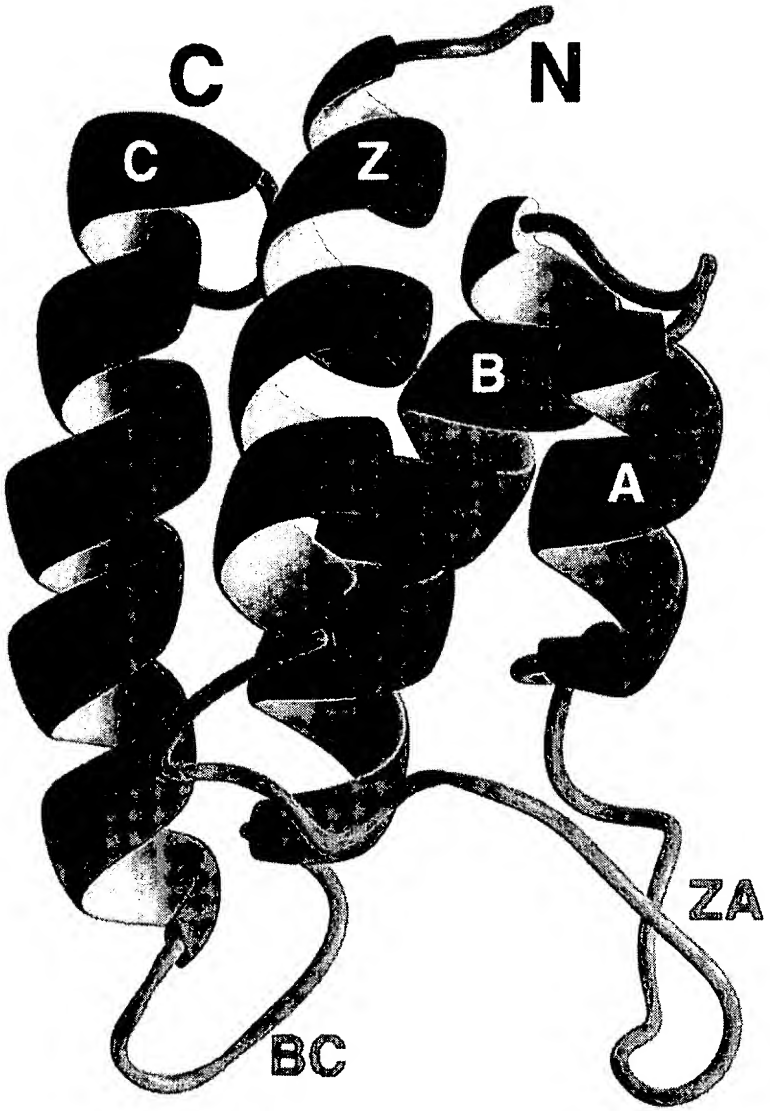

d

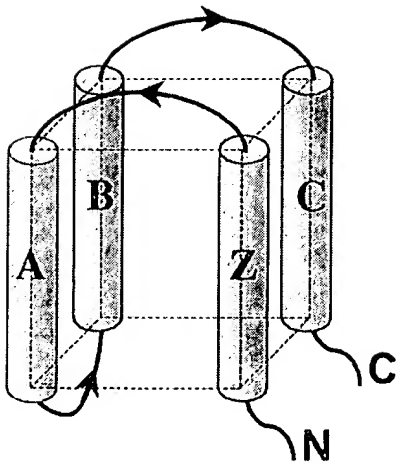

Left-handed bundle

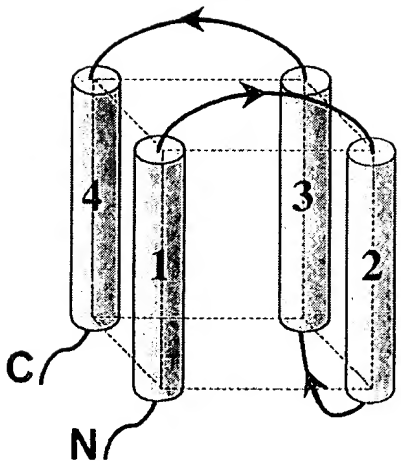

Right-handed bundle

e

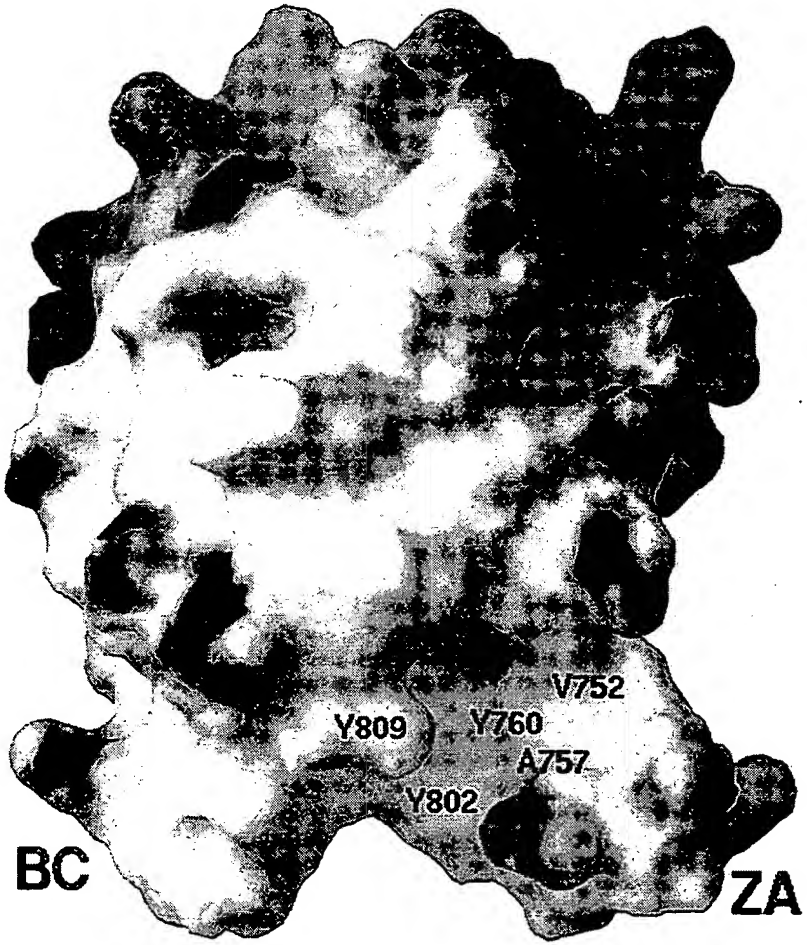

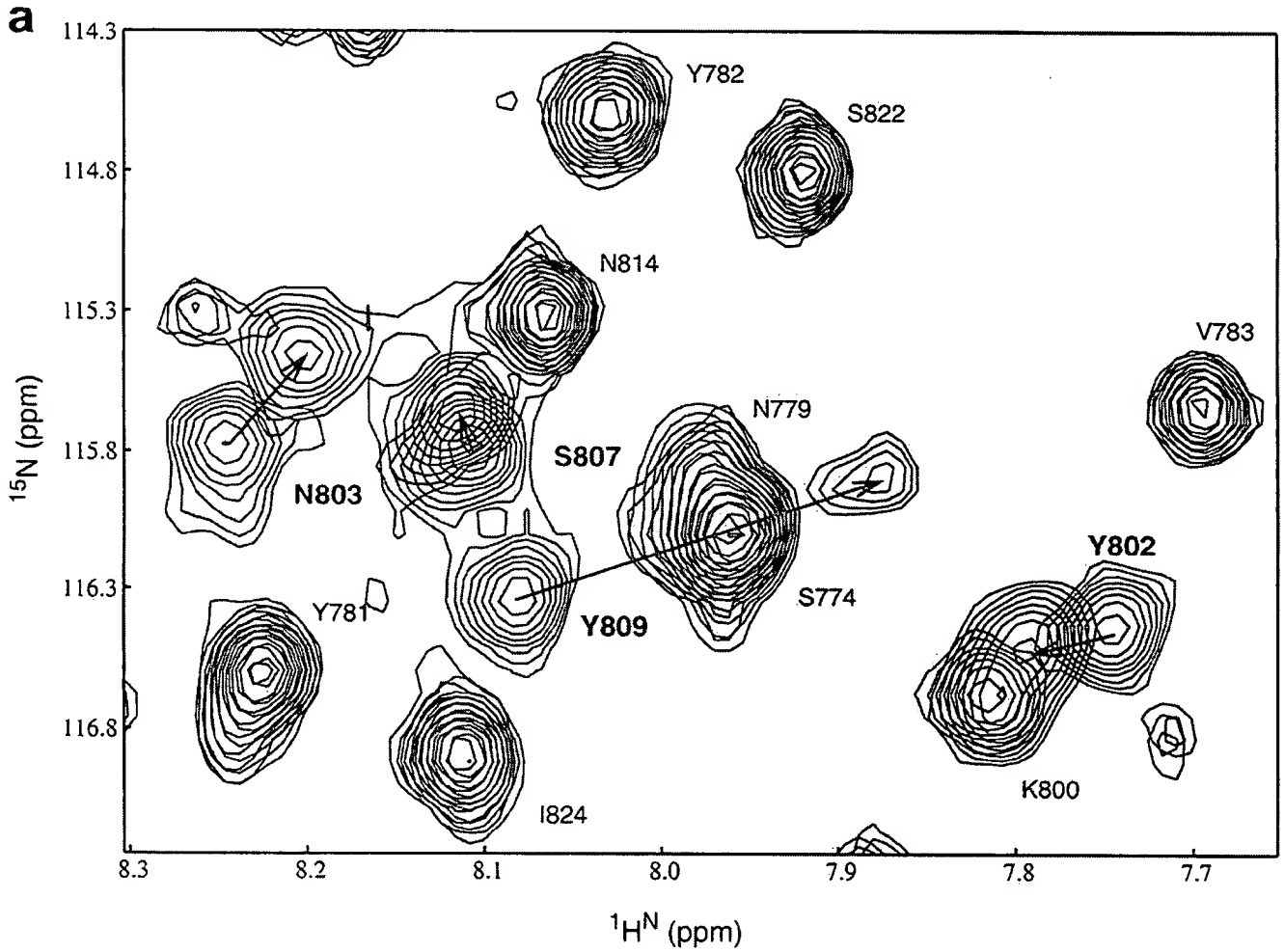
a
114.3
114.8
115.3
115.8
116.3
116.8
^{15}N (ppm)
8.3
8.2
8.1
8.0
7.9
7.8
7.7
^{1}H^{N} (ppm)
Y782
S822
N814
V783
N779
S807
N803
Y802
S774
Y781
Y809
K800
I824

b

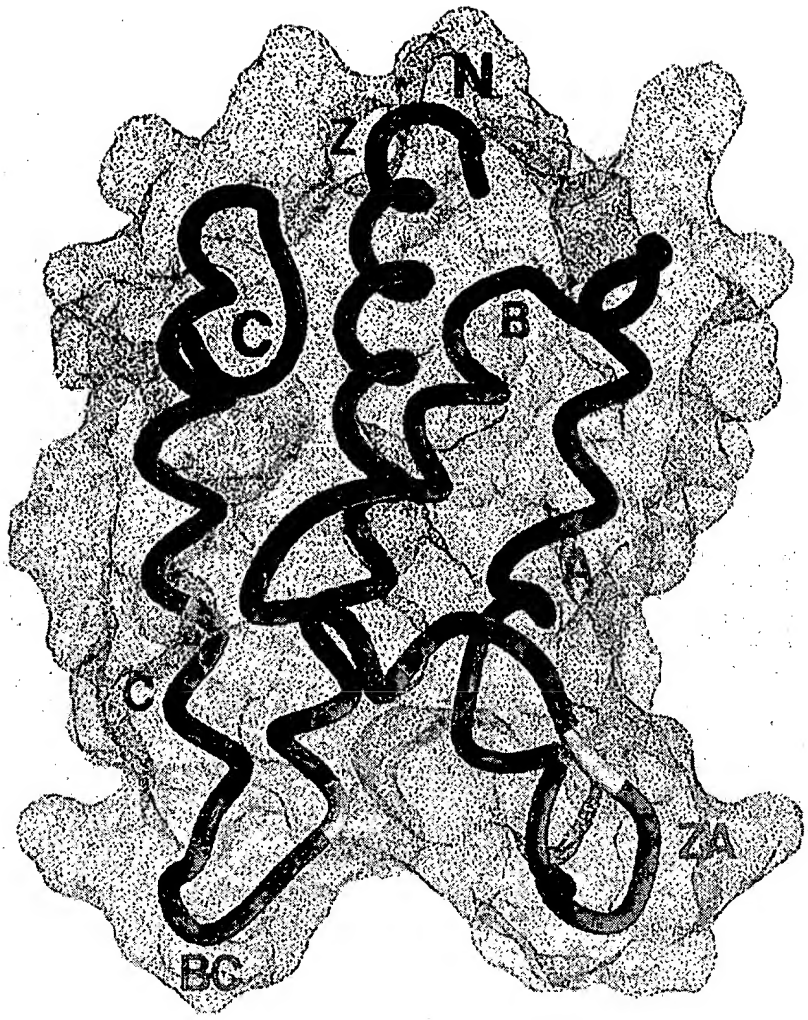

c

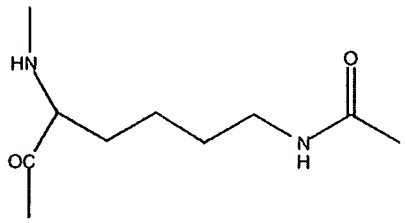

Nε-Acetyl-Lysine

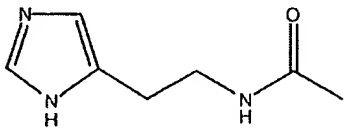

Nω-Acetyl-Histamine

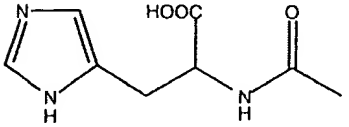

Nα-Acetyl-Histidine

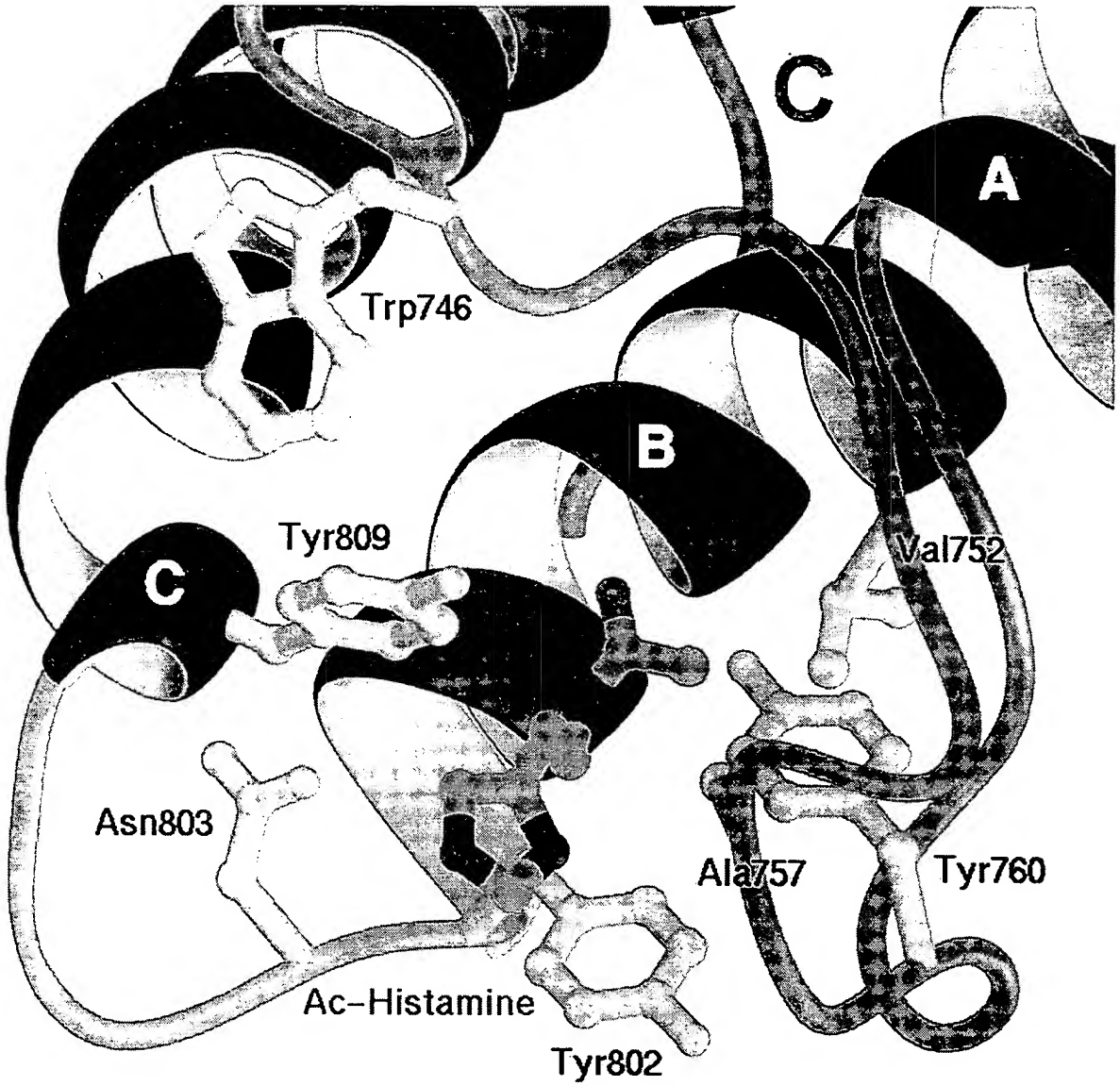
C
A
Trp746
B
Tyr809
C
Val752
Asn803
Ala757
Tyr760
Ac-Histamine
Tyr802

EXHIBIT "C"

/bloch2/chris/BROMO_XPLOR_ARIA32/structures/it8/

	Energies							Violations	
Conf	Total	Bond	Ang	Impr	VdW	NOE	DIH	NOE	DIH
1	149.29	8.99	74.37	0.00	21.43	30.32	0.25	1	0
2	156.15	8.82	75.95	0.00	21.65	34.02	0.23	1	0
3	156.61	9.53	72.66	0.00	22.48	35.64	0.20	1	0
4	157.92	9.31	73.15	0.00	23.18	36.43	0.23	2	0
5	162.14	9.61	71.78	0.00	25.02	38.60	0.41	1	0
6	165.75	10.96	79.55	0.00	22.04	37.10	0.33	1	0
7	169.06	10.23	77.32	0.00	25.00	38.57	0.36	2	0
8	170.88	10.28	77.62	0.00	23.95	43.29	0.24	2	0
9	172.70	10.08	77.44	0.00	26.26	42.00	0.38	2	0
10	175.65	11.37	80.83	0.00	26.92	38.55	0.57	2	0
11	175.66	10.49	77.43	0.00	32.21	39.10	1.33	1	0
12	176.67	12.32	79.77	0.00	23.03	45.73	0.13	2	0
13	177.33	10.12	84.45	0.00	26.78	34.95	0.41	2	0
14	179.11	11.39	74.75	0.00	26.24	47.07	0.69	1	0
15	179.84	11.11	81.68	0.00	31.00	37.26	0.41	2	0
16	180.69	10.82	81.81	0.00	24.53	44.19	0.44	2	0
17	180.71	11.15	84.32	0.00	25.03	39.64	0.54	1	0
18	183.25	10.93	84.00	0.00	26.15	42.73	0.47	2	0
19	185.33	11.17	85.23	0.00	26.98	43.93	0.44	2	0
20	186.00	11.60	86.04	0.00	27.75	43.27	0.55	2	0
21	187.42	11.74	79.70	0.00	29.39	45.70	0.20	3	0
22	187.66	11.97	83.74	0.00	31.43	40.65	0.21	2	0
23	187.82	11.44	81.15	0.00	25.38	49.06	0.82	2	0
24	188.46	12.29	82.43	0.00	26.29	48.08	1.79	4	0
25	190.85	11.82	81.73	0.00	31.44	47.73	0.57	2	0
26	190.94	11.82	95.87	0.00	27.40	37.80	0.35	2	0
27	195.68	11.92	89.81	0.00	26.70	43.20	0.93	3	0
28	196.07	11.86	86.45	0.00	28.68	45.85	0.37	3	0
29	197.00	13.16	86.02	0.00	30.01	47.93	0.70	2	0
30	197.65	12.40	83.64	0.00	31.95	49.67	0.55	5	0

RMSD for 30 conformations brd along the entire molecule (9-116)
average rms diff. to the mean struct. for the backbone= 0.626129 +/- 0.113342
average rms diff. to the mean struct. for non-h atoms= 1.14798 +/- 0.12386

RMSD for 30 conformations brd along the secondary structure elements (13-29;56-62;71-88;93-113)
average rms diff. to the mean struct. for the backbone= 0.33926 +/- 3.744659E-02
average rms diff. to the mean struct. for non-h atoms= 0.87368 +/- 5.579731E-02

Final Energies (kcal/mol)
E Total = 178.676 +/- 2.35547
E bonds = 11.0233 +/- 0.19469
E angles = 81.023 +/- 0.958855
E VdW = 26.5433 +/- 0.564117
E NOE = 41.602 +/- 0.898896
E dihedral = 0.503333 +/- 0.0627522

```
/bloch2/chris/BROMO_XPLOR_ARIA32/structures/it8/ambig.tbl
/bloch2/chris/BROMO_XPLOR_ARIA32/structures/it8/unambig.tbl

Total Restraints                  3515
Total NOE Restraints              3461
Total Ambigous NOE Restraints      590

Total Unambigous NOE Restraints   2843
Intraresidue                      1077    (37.88%)
Interresidue                      1766    (62.12%)
Sequential (|i-j|=1)               621    (21.84%)
Medium                             550    (19.35%)
             i,i+2                 128    (4.50%)
             i,i+3                 304    (10.69%)
             i,i+4                 118    (4.15%)
Long (|i-j|>4)                     595    (20.93%)
Hydrogen Bond Restraints            28
Dihedrals PHI                       54

%%%%%%%%%%%%%%%%%%%%%%%%%%%%%%%%%%%%%%%%%%%%%%%%%%%%
Manually assigned NOE table used to get starting structures with regular XPLOR
NOE distance restraints
All                               1324
Intraresidue                       495    (37.39%)
Interresidue                       829    (62.61%)
Sequential (|i-j|=1)               425    (32.10%)
Medium                             266    (20.09%)
             i,i+2                  58    (4.38%)
             i,i+3                 167    (12.61%)
             i,i+4                  41    (3.10%)
Long (|i-j|>4)                     138    (10.42%)
Hydrogen Bond Restraints            28
Dihedrals PHI                       54

%%%%%%%%%%%%%%%%%%%%%%%%%%%%%%%%%%%%%%%%%%%%%%%%%%%
PROCHECK analysis For 30 structures
For 30 structures
brd_fig_1 64.5 core 27.1 allow 5.6 gener 2.8 disall
brd_fig_2 69.2 core 21.5 allow 4.7 gener 4.7 disall
brd_fig_3 64.5 core 27.1 allow 4.7 gener 3.7 disall
brd_fig_4 66.4 core 28.0 allow 2.8 gener 2.8 disall
brd_fig_5 64.5 core 29.9 allow 3.7 gener 1.9 disall
brd_fig_6 69.2 core 27.1 allow 1.9 gener 1.9 disall
brd_fig_7 64.5 core 30.8 allow 1.9 gener 2.8 disall
brd_fig_8 64.5 core 29.9 allow 5.6 gener 0.0 disall
brd_fig_9 66.4 core 28.0 allow 3.7 gener 1.9 disall
brd_fig_10 65.4 core 29.9 allow 2.8 gener 1.9 disall
brd_fig_11 69.2 core 25.2 allow 3.7 gener 1.9 disall
brd_fig_12 69.2 core 24.3 allow 2.8 gener 3.7 disall
brd_fig_13 66.4 core 26.2 allow 3.7 gener 3.7 disall
brd_fig_14 63.6 core 29.0 allow 4.7 gener 2.8 disall
brd_fig_15 60.7 core 32.7 allow 3.7 gener 2.8 disall
brd_fig_16 66.4 core 27.1 allow 3.7 gener 2.8 disall
brd_fig_17 69.2 core 25.2 allow 2.8 gener 2.8 disall
brd_fig_18 61.7 core 29.9 allow 5.6 gener 2.8 disall
brd_fig_19 64.5 core 27.1 allow 3.7 gener 4.7 disall
brd_fig_20 66.4 core 29.0 allow 3.7 gener 0.9 disall
brd_fig_21 65.4 core 27.1 allow 2.8 gener 4.7 disall
brd_fig_22 60.7 core 33.6 allow 1.9 gener 3.7 disall
brd_fig_23 77.6 core 17.8 allow 3.7 gener 0.9 disall
brd_fig_24 68.2 core 24.3 allow 4.7 gener 2.8 disall
brd_fig_25 65.4 core 28.0 allow 4.7 gener 1.9 disall
brd_fig_26 67.3 core 27.1 allow 1.9 gener 3.7 disall
brd_fig_27 63.6 core 29.9 allow 2.8 gener 3.7 disall
brd_fig_28 63.6 core 29.9 allow 4.7 gener 1.9 disall
brd_fig_29 67.3 core 27.1 allow 3.7 gener 1.9 disall
brd_fig_30 68.2 core 23.4 allow 6.5 gener 1.9 disall

   Favoured Regions            = 66.1233 +/- 0.582804
   Additional Allowed Regions = 27.44 +/- 0.573267
   Generously Allowed Regions = 3.76333 +/- 0.216973
```



```
   Disallowed Regions         = 2.68 +/- 0.204418

PROCHECK analysis For 15 structures
For 15 structures
brd_fig_5 64.5 core 29.9 allow 3.7 gener 1.9 disall
brd_fig_6 69.2 core 27.1 allow 1.9 gener 1.9 disall
brd_fig_7 64.5 core 30.8 allow 1.9 gener 2.8 disall
brd_fig_8 64.5 core 29.9 allow 5.6 gener 0.0 disall
brd_fig_9 66.4 core 28.0 allow 3.7 gener 1.9 disall
brd_fig_10 65.4 core 29.9 allow 2.8 gener 1.9 disall
brd_fig_11 69.2 core 25.2 allow 3.7 gener 1.9 disall
brd_fig_17 69.2 core 25.2 allow 2.8 gener 2.8 disall
brd_fig_20 66.4 core 29.0 allow 3.7 gener 0.9 disall
brd_fig_23 77.6 core 17.8 allow 3.7 gener 0.9 disall
brd_fig_24 68.2 core 24.3 allow 4.7 gener 2.8 disall
brd_fig_25 65.4 core 28.0 allow 4.7 gener 1.9 disall
brd_fig_28 63.6 core 29.9 allow 4.7 gener 1.9 disall
brd_fig_29 67.3 core 27.1 allow 3.7 gener 1.9 disall
brd_fig_30 68.2 core 23.4 allow 6.5 gener 1.9 disall

For 15 structures
   Favoured Regions            = 67.3067 +/- 0.855282
   Additional Allowed Regions = 27.0333 +/- 0.857524
   Generously Allowed Regions = 3.85333 +/- 0.314093
   Disallowed Regions         = 1.82 +/- 0.187901
```